

Environmental Research

Stream sediments pollution: a compositional baseline assessment – the Caveira mine, Portugal

--Manuscript Draft--

Manuscript Number:	ER-23-9416
Article Type:	Research paper
Section/Category:	Environmental Health & Risk Assessment
Keywords:	Caveira mine; Pollution; Compositional Pollution Indicator (CPI); Sequential Gaussian Simulation; Probability map.
Corresponding Author:	Teresa Albuquerque, Ph.D Castelo Branco, PORTUGAL
First Author:	Teresa Albuquerque, Ph.D
Order of Authors:	Teresa Albuquerque, Ph.D Rita Fonseca Joana Araújo Natália Silva António Araújo
Abstract:	A high concentration of Potentially Toxic Elements (PTEs) can affect ecosystem health in many ways. It is therefore essential that spatial trends of pollutants are assessed and controlled. Two questions must be addressed when quantifying pollution. How to define a non-polluted sample? and, how to reduce the problems' dimensionality. Since the concentration of chemical elements is compositional, a compositional approach was used as the attributes vary together. A novel Compositional Pollution Indicator (CPI) based on Compositional Data (CoDa) principles such as sparsity and simplicity as properties, was computed. A dataset of 33 stream-sediment samples was collected from within 0 to 10 cm depth, in a grid of 1Km x 1Km, and twelve chemical elements were analyzed. Concentrations, reaching 3.8% Pb, 750µgg-1 As, and 340 µgg-1 Hg, were obtained near the mine tailings. The methodological approach implied the geological background selection in terms of a trimmed subsample that can be assumed as non-pollutant (Al and Fe) and the selection of a list of pollutants based on expert knowledge criteria and previous studies (As, Zn, Pb, and Hg). Finally, a sequential stochastic Sequential Gaussian Simulation was performed on the new CPI. The results of the performed hundred simulations are summarized through the mean image maps and the probability maps of exceeding a given statistical threshold, thus, allowing the characterization of the spatial distribution and associated variability of the CPI. A better understanding of the trends of relative enrichment and PTEs' fate is discussed.
Suggested Reviewers:	Carlos Boente, Ph.D Assistant Professor, Autonomous University of Madrid carboente@gmail.com Dr. Carlos Boente has been working on pollution and risk assessment, namely related to old mining and industrial areas. Catarina Silva, Ph.D Assistant Professor, University of Lisbon csilva@fc.ul.pt Dr. Catarina Silva has been working in water pollution and water supply focusing in urban and industry contributions. José Luís Gallego, Ph.D Full Professor, University of Oviedo jgallego@uniovi.es Dr. Gallego is an expert in Geochemistry and Environmental Engineering, namely, soil remediation.

Pedro Proença e Cunha, Ph.D
Full Professor, University of Coimbra
pcunha@dct.uc.pt
Dr. Proença e Cunha has been working in hazard monitoring related to old mining areas.

Carlos Sierra, Ph.D
University of León
sierrafernandezcarlos@gmail.com
Dr. Sierra is an expert in Environmental Engineering and Chemical Engineering, namely related to old mining and industrial areas.

Alexandre Tavares, Ph.D
Associate Professor, University of Coimbra
atavares@ci.uc.pt
Dr. Tavares has been working in environmental risk assessment.

Castelo Branco, 25 August 2023.

Dear Prof. Dr., José L. Domingo

I hereby submit to the journal Environment Research the manuscript entitled “Stream sediments pollution: a compositional baseline assessment – the Caveira mine, Portugal”. The manuscript tackles an important topic regarding natural hazards namely what concerns a better understanding of the trends of relative enrichment and Potentially Toxic Elements (PTE) fate related to old mining activities. The methodological approach developed can be easily applied to other areas under acid waters’ drainage and is a key support tool for decision-makers.

All authors have seen and accepted the manuscript's contents. The submitted manuscript describes the original work and we all confirm that results have not been published elsewhere and are not under consideration by another journal.

Yours sincerely,



Teresa Albuquerque
(Correspondent author)

Highlights

- ❖ A high concentration of Potentially Toxic Elements (PTEs) can affect ecosystem health in many ways
- ❖ Two questions must be addressed when quantifying pollution. How to define a non-polluted sample? and, how to reduce the problems' dimensionality
- ❖ A novel Compositional Pollution Indicator (CPI) based on Compositional Data (CoDa) was computed
- ❖ Sequential Gaussian Simulation was performed on the new CPI and probability maps of exceeding a given statistical threshold computed

1 **Stream sediments pollution: a compositional baseline assessment – the
2 Caveira mine, Portugal**

4 Teresa Albuquerque^{1,2,3*}, Rita Fonseca³, Joana Araújo³, Natália Silva³, António Araújo³

5 ¹ Instituto Politécnico de Castelo Branco, Av. Pedro Álvares Cabral, nº 12, 6000-084 Castelo Branco,
6 Portugal.

7 ² Centro de Estudos de Recursos Naturais, Ambiente e Sociedade (CERNAS) - Instituto Politécnico de
8 Castelo Branco, Av. Pedro Álvares Cabral, nº 12, 6000-084 Castelo Branco, Portugal.

9 ³ ICT| Universidade de Évora, Largo dos Colegiais 2, 7000 Évora, Portugal.

10 **Abstract**

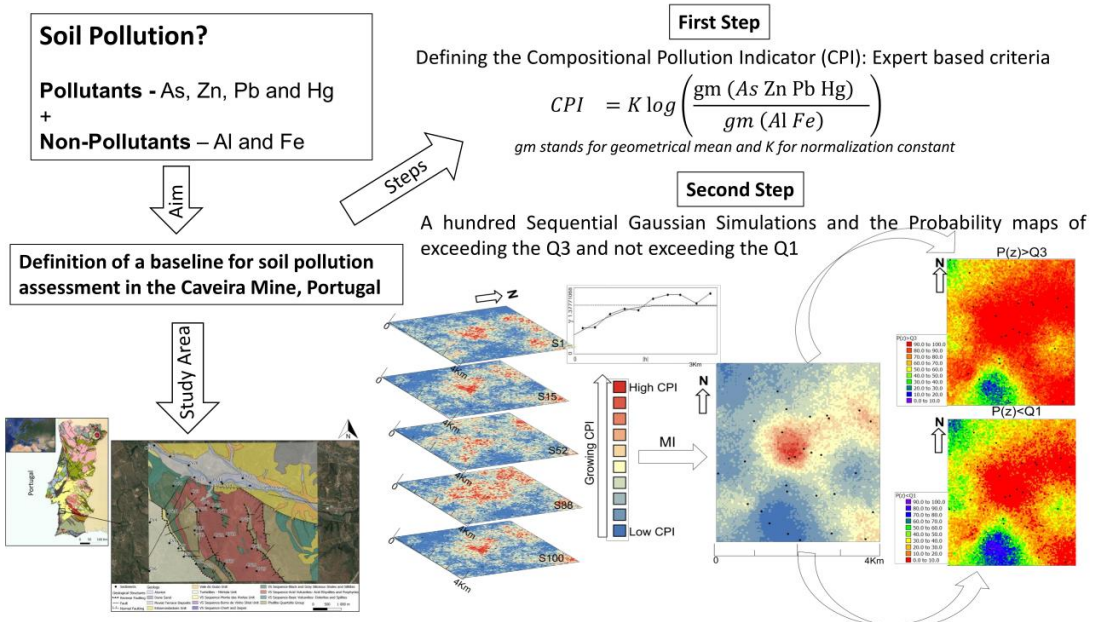
11 A high concentration of Potentially Toxic Elements (PTEs) can affect ecosystem health
12 in many ways. It is therefore essential that spatial trends of pollutants are assessed and
13 controlled. Two questions must be addressed when quantifying pollution. How to define
14 a non-polluted sample? and, how to reduce the problems' dimensionality. Since the
15 concentration of chemical elements is compositional, a compositional approach was
16 used as the attributes vary together. A novel Compositional Pollution Indicator (CPI)
17 based on Compositional Data (CoDa) principles such as sparsity and simplicity as
18 properties, was computed. A dataset of 33 stream-sediment samples was collected from
19 within 0 to 10 cm depth, in a grid of 1Km x 1Km, and twelve chemical elements were
20 analyzed. Concentrations, reaching 3.8% Pb, 750µgg-1 As, and 340 µgg-1 Hg, were
21 obtained near the mine tailings. The methodological approach implied the geological
22 background selection in terms of a trimmed subsample that can be assumed as non-
23 pollutant (Al and Fe) and the selection of a list of pollutants based on expert knowledge
24 criteria and previous studies (As, Zn, Pb, and Hg). Finally, a sequential stochastic
25 Sequential Gaussian Simulation was performed on the new CPI. The results of the
26 performed hundred simulations are summarized through the mean image maps and the
27 probability maps of exceeding a given statistical threshold, thus, allowing the
28 characterization of the spatial distribution and associated variability of the CPI. A better
29 understanding of the trends of relative enrichment and PTEs' fate is discussed.

30 **Key Words:** Caveira mine; Pollution; Compositional Pollution Indicator (CPI); Sequential
31 Gaussian Simulation; Probability map.

32
33
34 *Corresponding author.

35 E-mail address: teresal@ (M-T.D. Albuquerque)

41 Graphical Abstract



44 **1. Introduction**

45 Potentially toxic elements (PTE) constitute a significant liability in different environmental
46 sectors. Over the past decades, the cumulative environmental impact has been
47 enormous. The problem of PTEs in stream sediments has led during the time to an
48 exponential concentration increase and, therefore, exceeded the human and
49 environmental risks (Antoniadis et al., 2017; Kumudunis et al., 2020). Mining and heavy
50 industrial activities may potentiate these high observed levels of PTEs and be the origin
51 of numerous sources of contamination (Boente et al., 2022, Carvalho et al. 2022, Boente
52 et al., 2018). Thus, in recent decades, researchers have invested in the development of
53 new techniques to offer accurate scenarios of the spatial distribution of PETs. The
54 definition of geochemical backgrounds and the identification of enrichment sources are
55 key to the accomplishment of this objective (Wang et al., 2021; McKinley et al., 2016).
56 Visualization of spatial-temporal distribution models using simulated maps is an
57 important tool for the visualization and depiction of pollutants. The definition of
58 vulnerability and risk hot clusters may act as the basis for supporting environmental
59 policy-making in complex scenarios (Boente et al., 2020, Albuquerque et al., 2017,
60 McKinley et al., 2016). In the area of soil sediment science, a common strategy for
61 describing the distribution of PTEs is to map a single-component synthesis new variable
62 called indices or indicators. Unfortunately, usually, the compositional nature of the
63 geochemical data is considered (Pawlowsky-Glahn et al., 2015, Filzmoser et al., 2009,).
64 In most cases, these indicators are related to the study of individual elements, without
65 considering the existing dependence between the concentrations of all elements in the
66 same set. usually use The non-compositional indices often used to study geochemical
67 data are the Geoaccumulation Index (Muller, 1969), the Enrichment Factor (Sucharova
68 et al., 2012), or the Single Pollution Index (SPI) (Hakanson, 1980), reviewed in Kowalska
69 et al. (2018). Nevertheless, it is well known that a traditional statistical approach using
70 direct raw data can be misleading (Chayes 1962, 1971). Aitchison and his fundamental

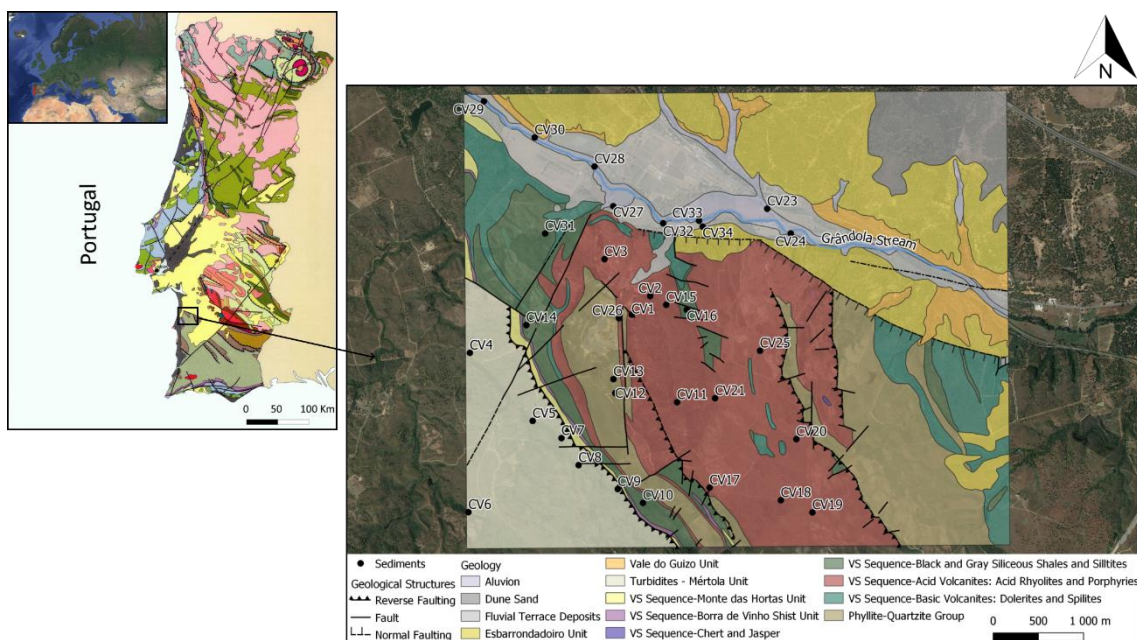
71 work on the method of logarithmic ratio (1982, 1986) answered these questions.
72 Theories of composition data (CoDa) have enhanced the understanding of the sampling
73 space of composition data and their corresponding structure (Pawlowsky-Glahn and
74 Egozcue 2001). Representations of data considering pairwise log ratios (pwlr), isometric
75 lg-ratio coordinates (ilr), centered log-ratio coordinates (clr), and additive log-ratio
76 coordinates (alr) are statistically robust approaches to deal with the compositional nature
77 of chemical concentration data (Pawlowsky-Glahn and Egozcue, 2001; Egozcue et al.,
78 2003; Buccianti and Grunsky, 2014). The compositional approach (CoDa) is well-
79 represented in various fields of research in environmental science, such as ecotoxicology
80 (Mullineaux et al., 2021), urban impacts (Cicchella et al., 2020), water quality
81 management (Wei et al., 2018), and human health (Tepanosyan et al., 2020, Pawlowsky-
82 Glahn and Buccianti, 2011; Filzmoser et al., 2021). Recently the adoption of
83 compositional indicators for PTEs soil pollution characterization is increasing (Boente et
84 al., 2022, Petrik et al., 2018). Compositional indicators involving geochemical baselines
85 definition offer a valuable contribution as they are scale-invariant and sub-
86 compositionally coherent, meaning that a change in the concentration's unit will not
87 modify the study's results (Pawlowsky-Glahn et al., 2015).
88 This research introduces a new Compositional Pollution Indicator (CPI) of riverine
89 sediments, built to characterize pollution in the Caveira mine in southern Portugal, using
90 the approach developed by Boente et al. (2022) corresponding to a balance of elements
91 chosen through expert criteria although respecting the same CoDa principles.

92 **2. Material and Methods**

93 **2.1 Characteristics of the study area and the data set**

94 The studied sector is part of the Portuguese Iberian Pyrite Belt and is an example of
95 post-mining European areas back to the 1990s. Mining activity ceased mainly because
96 of ore exhaustion and more profitable methods worldwide which resulted in ore price

97 reduction and made local mining activities infeasible (Martins and Oliveira, 2000).
 98 Therefore, major pollution problems related to metal dispersion and mine waste
 99 management are noteworthy. The geological sequence at Caveira mine which closed
 100 back in the 1980s, corresponds from bottom to top to phyllites and quartzites (PQG),
 101 followed by a volcanic sedimentary complex sequence (VSC) unit (Late Famennian)
 102 represented by pyroclastics, rhyolitic lavas, tuffs, dark grey, and siliceous shales, and
 103 rare jaspers. Intruding diabase rocks are spotted in the northern sector. (Fig. 1). The
 104 massive sulfide deposits that were exploited in the region occurred in the vicinity of felsic
 105 volcanic rocks. The Mértola formation with Visean age, overlays the CVS and
 106 corresponds to a flysch sequence, consisting of sandstones alternating with shales and
 107 thin-bedded siltstones. From a structural point of view, the whole sequence is part of the
 108 South Portuguese Zone, a thin-skinned fold and thrust belt, with Variscan age. Tailings,
 109 and associated waste rock, resulting from 129 years of pyrite and Cu mining, are
 110 scattered along the Grândola Creek. The semi-arid climatic conditions encompass high
 111 erosion of residues by surface water, primarily during rainfall, causing serious
 112 contamination of the Grândola stream and its tributaries, conducted to the degradation
 113 of sediments (Ferreira da Silva et al, 2015).



114

115 **Fig 1.** Study area and collected sample's location.

116 A dataset of 33 bottom sediment samples distributed over small and narrow creeks two
117 of them flowing by the mine tailings pile and the larger Grândola stream, of which they
118 are tributaries. These streams belong to the Sado River Basin, the second-largest
119 hydrographical basin in Southern Portugal. Samples were collected from within 0 to 10
120 cm depth with an environmental hand soil sampling kit (#209.55, AMS), in a grid of 1Km x
121 1Km and twelve chemical elements, including PTEs of variable toxicity (As, Cd, Co, Cr,
122 Hg, Mn, Ni, Pb, Zn, V) and major elements from lithogenic sources (Fe, Al), were
123 analyzed in preserved samples at about 4°C. The most extractable forms of metals
124 (except for Hg) were obtained by partial digestion with aqua regia (HCl and HNO₃) in a
125 high-pressure microwave digestion unit (Anton Paar Multiwave PRO) following the US
126 EPA (2007) Method 3051A. Metals and As were analyzed by optical emission
127 spectroscopy with an inductive plasma source (ICP-OES, Perkin-Elmer OPTIMA 8300),
128 using yttrium as an internal standard. The accuracy and analytical precision of all the
129 analyses have been checked by the analysis of reference materials and duplicate
130 samples in each analytical set.

131 Mercury (Hg) was analyzed by a mercury analyzer (NIC MA-3000) based on thermal
132 decomposition, gold amalgamation, and cold vapor atomic absorption spectroscopy
133 detection. Sampling was followed by immediate readings of pH and redox potential
134 values in wet samples, using a portable multi-parameter Consort, C5020 (SP10T model
135 for pH, SP50X model for redox potential). In samples with insufficient moisture for direct
136 pH readings, this parameter was measured in water–sediment suspension (2.5:1), in the
137 laboratory. Respecting to samples' chemistry, the dataset includes PTEs of variable
138 toxicity (Fabian et al., 2014). The set of 12 elements was reported across the 33 sampling
139 points, resulting in a 12-part composition that is assumed to represent the stream
140 sediments.

141 **2.2 Compositional Pollution Indicator (CPI) construction**

142 The first fundamental principles of composition data are to be found in the founding work
143 of Aitchison (1986). These initial contributions are explained and expanded into general-
144 purpose works such as Pawlowsky-Glahn et al. (2015); Boogaart van den and Tolosana-
145 Delgado (2013); Filzmoser and Hron (2011); Pawlowsky-Glahn and Buccianti (2011) and
146 Pawlowsky-Glahn and Serra (2019).

147 The analysis of a stream sediment sample, given by its chemical composition should be
148 conducted under the assumption that these data are compositional. As a result, when
149 performing data analysis, the functions used to describe the composition should be
150 invariant under multiplication by a positive constant (Boente et al., 2022). Also, any
151 composition can be expressed in proportions (components adding to 1) without adding
152 or losing any information, irrespective of the units in which the data were initially
153 represented.

154 The chemical composition of a sample of riverine sediments in units such as mg/kg
155 should be performed assuming that these data are compositional. Moreover, the
156 conversion of units from mg/kg to g/kg, as an example, must not change the information
157 in the sample. This is summed up in one of the principles of CoDa analysis, named the
158 Principle of Scale Invariance. Thus, when analyzing the data, the functions used to
159 describe the composition should be invariantly multiplied by a positive constant.
160 Consequently, any composition can be expressed in proportions (components adding 1)
161 without adding or losing information regardless of the units in which the data were
162 originally reported. A second assumption is known as Sub compositional Coherence
163 Principle. The whole periodic table is never presented, only a subset of elements is
164 measured, and this subset may change in time and the field. The elements observed
165 form a composition and any subassembly of the same is a sub-composition, again
166 subject to the Principle of Scale Invariance. Analyses of initial composition or sub-

167 composition should lead to coherent conclusions describing the role of common
 168 elements (Aitchison, 1986)

169 The CPI balance was obtained based on expert criteria attending a selection of elements
 170 (Boente et al., 2022), of which some are considered pollutants while others are not. In
 171 the case of the Caveira mine, the main contaminants were selected from typical
 172 pollutants namely, As, Zn, Pb, and Hg, while Al and Fe were selected as the main natural-
 173 source elements (or non-pollutants). Based on this previous study, the selected balance,
 174 CPI, was constructed as follows:

$$175 \quad CPI = \sqrt[3]{\frac{4}{3} \ln \left(\frac{(As \ Zn \ Pb \ Hg)^{1/4}}{(Al \ Fe)^{\frac{1}{2}}} \right)} \quad (1)$$

176 **2.3 Spatial modeling – geostatistical approach**

177 The computed Compositional Pollution Indicator (CPI) is unbounded, a real random
 178 variable. Therefore, it fulfills the assumptions underlying a conventional geostatistical
 179 approach. Their spatial probability patterns were computed following a two-step
 180 geostatistical modeling method: 1. Structural analysis and experimental variograms
 181 computation (Journel and Huijbregts, 1978) followed by 2. Sequential Gaussian
 182 Simulation (SGS) is used as a stochastic simulation algorithm over a 100x100 Km grid
 183 mesh.

184 The new CPI can be considered a Regionalized variable (Matheron, 1971) as it depends
 185 on the spatial location determined by the coordinates and is additive by construction.
 186 Indeed, the mean value within a given observed support is equal to the arithmetic
 187 average of the sample values, independently of the associated statistical distribution
 188 (Albuquerque et al., 2017; Rivoirard, 2005). Thus, the vector function used to calculate
 189 the spatial variation structure was the semi-variogram (Journel & Huijbregts, 1978).

$$190 \quad \gamma(h) = \frac{1}{2N(h)} \sum_{i=1}^{N(h)} [Z(x_i) - Z(x_i + h)]^2 \quad (2)$$

191 The arguments taken into consideration are h (distance) where $Z(x_i)$ and $Z(x_i+h)$ are the
192 numerical values of the variables assigned to x_i and x_i+h . The total number of couples at
193 a specified distance of h is $N(h)$. Therefore, it is the average value of the square of the
194 differences between all couples of points existing in the geometric field spaced at an h
195 distance (Journel and Huijbregts, 1978). Plotting the behavior of the variogram gives an
196 overall view of the spatial structure of the variable. One of the parameters that provide
197 this information is the nugget (C_0) effect, which supplies the behavior at the origin. The
198 two other parameters are the sill (C_1) and the amplitude (a) which define correspondingly
199 the inertia used in the subsequent interpolation process and the influence radius of the
200 variable.

201 The SGS starts by computing the univariate experimental distribution of values and
202 performing a normal score transformation of the original values to a standard normal
203 distribution (Goovaerts, 1997). Normal scores at grid node locations are then simulated
204 sequentially with simple kriging (SK) using the normal score data and a zero mean. Once
205 all normal scores have been simulated, they are back-transformed to their original units.
206 The outcome of a simulation is always a random version of the estimation process,
207 reproducing the statistics of the known data and building a realistic picture of reality. The
208 associated spatial uncertainty is visualized through the construction of probability maps
209 If multiple sequences of simulation are computed, it is possible to obtain reliable
210 probabilistic maps. The mean image and the Probability maps of exceeding the third
211 quartile (Q_3) and not exceeding the first quartile (Q_1) were computed.

212 **3. Results and Discussion**

213 **3.1 Geochemical data**

214 The analyses of physicochemical parameters, and the determination of the levels of
215 PTEs of variable toxicity (As, Cd, Co, Cr, Hg, Mn, Ni, Pb, Zn, V) as well as the selected
216 elements from lithogenic sources (Fe, Al), were evaluated considering their capacity of

217 solubilization and mobilization aiming contamination mapping. The evaluation of the
218 metal's mobility was based on partial digestion analysis (using *Aqua Regia*) considering
219 the pH values. The element concentrations and pH values in the stream sediment
220 samples are reported in Table 1. Considering the physical-chemical parameter that most
221 affects the solubility, mobility, and precipitation of potentially toxic metals in the
222 sediments from shallow streams, pH, values range from 2.06 and 7.39, corresponding
223 to the lower values (2.06-4.57) to the sediments from the 2 creeks flowing through the
224 mining tailings pile. As would be expected, these sediments (Cv1, Cv2, Cv3, Cv26, Cv
225 33, Cv34) are those with the highest values of Pb, As, and Hg, the main contaminants in
226 the mine tailings that reach levels above those considered critical and which require
227 immediate intervention, according to the European Regulations (based on the
228 Netherlands legislation – Soil Quality Regulation, 2006). Zn, another element with levels
229 of concern, and which represents one of the elements with high contents in the massive
230 sulphides that have been exploited in this mine, presents slightly contaminating levels in
231 all the diffused streams flowing from the tailings pile, mostly in locations that do not
232 coincide with the locations where the other elements have exceeded critical levels. The
233 highest values of this element also do not coincide with the most acidic conditions of the
234 environment. Although any of these elements originate from the ores that were exploited
235 in this mining area, Zn is an element with higher chemical mobility, and because this
236 mobility is mostly influenced by the oxidation conditions that occurred in all sediments
237 (240 – 650 mV), its distribution is more diffuse.

238

239

240

241

242

243
244**Table 1.** Element concentrations in the stream sediment samples (spring season) from Grândola,
and its tributary streams. These waterways belong to the Sado watershed.

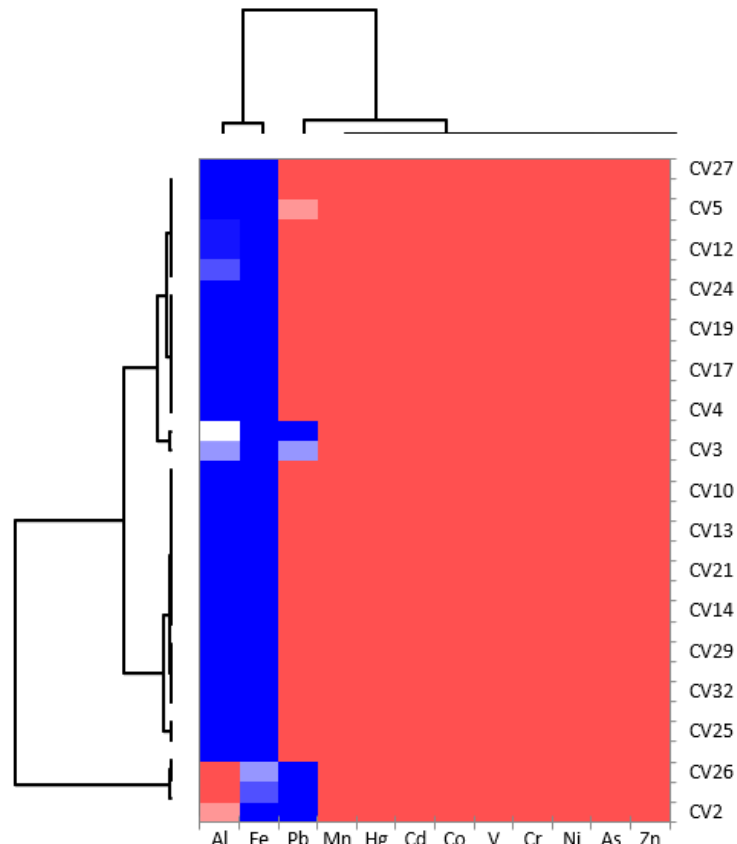
Samples * (mg/Kg)	As	Cd	Co	Cr	Mn	Ni	V	Zn	Al	Fe	Pb	Hg	pH (H ₂ O)
CV1	234,9	1,5	0,4	2,3	16,9	1,6	3,3	94,2	1441,6	10217,0	38458,7	127,9	2,30
CV2	238,6	< 0,5	0,4	1,6	24,5	1,0	2,0	96,4	2168,4	17815,8	29837,2	78,2	2,06
CV3	517,6	< 0,5	0,8	1,5	99,6	0,9	2,9	122,3	16128,4	65825,8	13775,3	125,8	4,57
CV4	< 1,5	< 0,5	3,9	13,3	172,7	10,3	14,3	36,4	18321,3	31828,4	51,2	1,7	6,61
CV5	14,7	< 0,5	3,5	15,6	261,9	12,7	15,5	47,2	13099,4	27183,4	2881,5	13,7	6,00
CV6	< 1,5	< 0,5	3,4	17,6	208,4	9,3	24,3	30,0	26272,6	21172,3	221,4	0,2	6,54
CV7	< 1,5	< 0,5	4,2	18,6	399,1	11,2	29,2	36,4	29376,6	28193,2	97,2	0,6	6,64
CV8	< 1,5	< 0,5	4,6	19,5	455,6	12,3	25,7	37,5	24811,4	28361,9	15,0	0,3	7,17
CV9	< 1,5	< 0,5	5,8	13,4	414,1	12,4	13,8	34,7	13007,8	27207,6	16,4	0,2	4,99
CV10	< 1,5	< 0,5	5,6	15	315	21,6	22,9	46,3	23727,5	23919,7	18,2	0,6	5,12
CV11	3,4	< 0,5	1,0	1,4	148	1,2	2,6	15,8	8807,1	12058,1	21,5	0,3	5,05
CV12	31,2	< 0,5	4,2	9,6	138,6	10,6	15,9	140,4	11176,5	29630,2	92,7	2,6	5,30
CV13	1,6	< 0,5	34,4	23,8	903	21,8	36,4	165,8	44359,5	42371,5	36,3	1,6	7,29
CV14	1,6	< 0,5	4,1	16,1	434,9	15,9	24,3	47,5	18683,1	21463,1	36,6	0,6	6,03
CV15	1,7	< 0,5	0,5	1,9	82,2	0,6	3,6	5,3	8882,1	3720,9	2,5	0,2	5,48
CV16	< 1,5	< 0,5	0,6	2,1	198,2	1,3	4,6	17,5	4821,9	5337,6	25,9	0,2	5,98
CV17	4,0	< 0,5	1,6	4,3	412,9	4,0	5,2	15,8	10396,1	16746,8	27,1	0,1	6,35
CV18	< 1,5	< 0,5	0,6	2,5	117,3	1,5	2,7	8,9	3475,2	3540,5	8,1	0,3	5,51
CV19	1,8	< 0,5	0,5	1,4	66,3	0,7	2,3	8,1	3044,8	3855,6	7,6	0,1	5,55
CV20	2,1	< 0,5	1,0	4,5	169,6	1,5	6,8	10,6	3677	5856,6	9,8	0,2	5,82
CV21	< 1,5	< 0,5	0,8	2,0	194,6	0,5	3,6	9,9	3574,9	3936,7	7,9	0,1	6,04
CV23	1,9	< 0,5	1,3	11,9	98,5	6,2	14,1	136,3	9503,4	9550,3	38,1	3,0	7,39
CV24	44,2	< 0,5	1,5	7,0	79,2	5,8	12,1	122,4	9728,8	13370,1	585,3	5,7	6,74
CV25	< 1,5	< 0,5	0,4	1,5	84,8	0	3,7	6,3	14787,2	7836,1	4,4	0,1	6,63
CV26	140,3	< 0,5	0,4	1,6	34,4	2,0	2,6	123,4	1193,7	10730,9	44540,5	46,8	2,34
CV27	32,3	< 0,5	3,6	11,6	177,5	12,5	17,9	129,0	13208,0	25540,5	82,8	7,3	6,39
CV28	< 1,5	< 0,5	3,7	16	385,5	10,1	24,6	36,0	22281,1	17596,5	29,1	1,3	5,34
CV29	< 1,5	< 0,5	3,9	18,4	394,6	10,7	25,6	36,2	22665,1	18556,6	14,5	0,2	6,82
CV30	< 1,5	< 0,5	4,1	13,8	258,4	11,8	15,9	39,8	11984,7	19370,5	21,5	0,1	6,16
CV31	9,0	< 0,5	2,1	14,2	106,4	10,5	15,7	30,2	6909,5	23545,1	31,0	0,2	6,21
CV32	30,8	< 0,5	3,4	15,7	291,3	8,9	24,6	88,6	24220,0	19152,6	107,7	2,3	6,57
CV33	265,2	< 0,5	3,9	9,3	422,5	8,6	11,6	108,2	11998,7	30136,3	88,8	1,6	4,26
CV34	748,2	< 0,5	0,4	8,3	77,6	3,9	10,8	161,8	6854,4	44363,4	23162,4	381,4	2,13

*Sample Cv22 was eliminated

245
246

Furthermore, a heat map was used for data exploratory analysis of the geochemical composition and sample clustering simultaneously in a synthetic way (Fig.2) ((Wilkinson and Friendly, 2009; Langella et al, 2013). The heat map observation shows the elements divided into two groups (upper dendrogram). The first one corresponds to Al and Fe (non-pollutants) and the second one corresponds to As, Cd, Co, Cr, Mn, Ni, V, Zn, Hg,

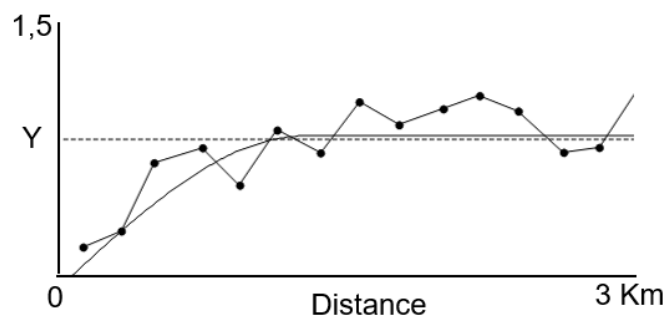
252 and Pb. This last element shows a distance within the major group. Based on an expert-
 253 driven approach As Zn Pb Hg were selected as pollutants. The samples dendrogram
 254 (left one). is divided into three groups The central group corresponds to samples Cv6;
 255 Cv8; Cv10; Cv13; C14; Cv16; Cv17; Cv18; Cv21; Cv23; Cv25; Cv28; Cv29 and Cv32;
 256 the left group to samples Cv1; Cv2; Cv15 and Cv26 and the right group to samples CV3;
 257 Cv4; Cv5; Cv9; Cv11; Cv12; Cv19; Cv20; Cv24 and Cv27; Cv30; Cv31; Cv33 and Cv34.
 258 The map represents values in the dataset re-arranged according to the dendograms.
 259 Focusing on rectangle/square patterns (from red to blue through a white increasing level
 260 of significance) inside the map it is possible to see, concerning the bottom group of
 261 samples Cv1; Cv2; Cv15, and Cv26, together with samples Cv34 and Cv3 of the upper
 262 group a lower significance cluster for Al and a higher significance cluster for Pb, relatively
 263 to the other samples. In future work, the relationship between the samples' geochemical
 264 print and the associated geology will be explored.



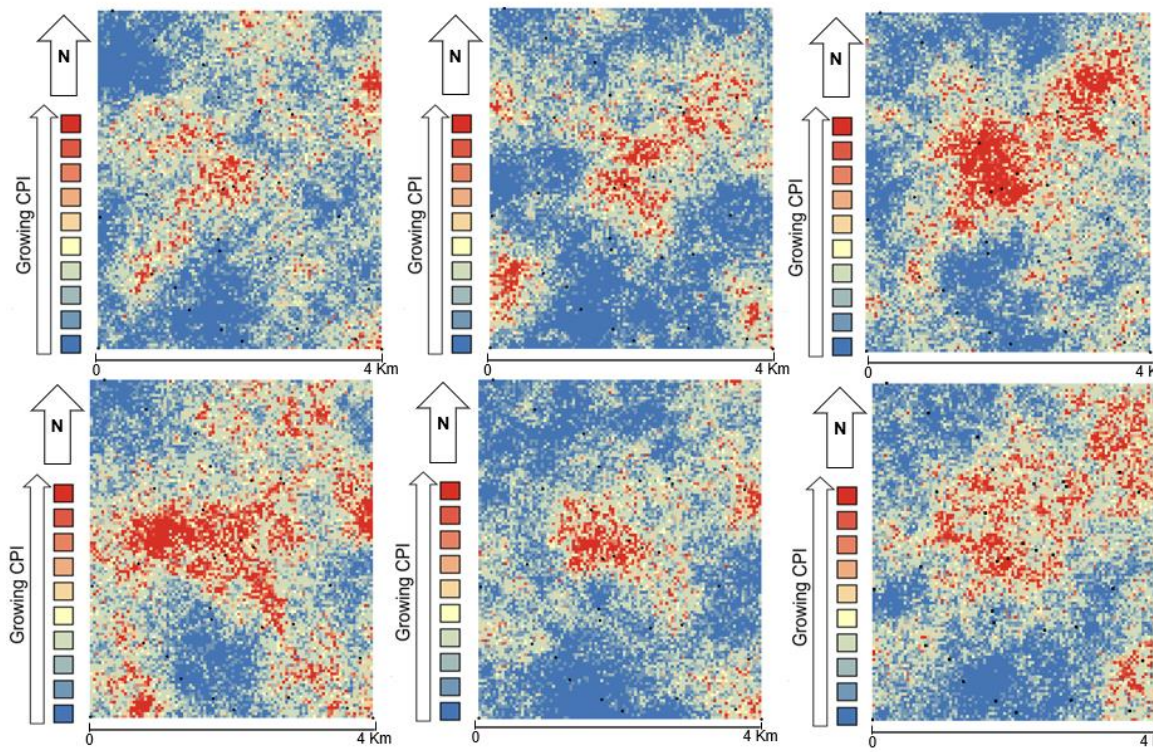
274 **Fig.2.** Heat map and simultaneously sample/geochemical print dendograms.

275 **3.2 The Compositional Pollution Indicator**

276 The compositional balance of the CPI was obtained according to expert criteria. These
277 criteria account for a selection of factors, some of which are considered pollutants while
278 others are not. In the case of the Caveira mine, the identification of the main pollutants
279 was addressed in previous studies (e.g. Ferreira da Silva et al, 2015), where typical
280 pollutants such as As, Zn, Pb, and Hg are identified as related to the Iberian Pyrite Belt
281 old mines activities. While the main natural-source elements (or non-pollutants) were
282 several major elements (i.e., Al and Fe). The CPI spatial modeling aimed at the definition
283 of hazardous clusters. Thus, a two-step geostatistical approach was used. The
284 experimental isotropic variogram was computed as no clear evidence of anisotropy was
285 found and the corresponding fitted model is shown in Fig. 2. Cross-validation correlation
286 index of the observed and estimated CPI values is 0.70 and, therefore, considered
287 satisfactory for the selected models. Furthermore, A hundred simulations were
288 performed using SGS as a conditional stochastic simulation of the CPI value distribution,
289 and a hundred equiprobable scenarios were computed.



290
291 **Fig.2.** Experimental and fitted spherical omnidirectional variogram.
292 Probability maps, corresponding to different thresholds allowed the visualization of
293 spatial variability setting aside the discussion of local accuracy and allowing the
294 identification of hot clusters of pollution in the subject area. The realization numbers 1,
295 15, 32, 52, 67 and 99 are shown in Fig.3.
296



310 **Fig.3.** Six different scenarios were obtained by Sequential Gaussian Simulation (SGS).

311 The problem is that all representations (scenarios) have the same reliability, which
 312 means that a single achievement cannot be seen as a better representation of reality.
 313 Therefore, the mean spatial images (MI) - average map – was computed and used as
 314 the CPI spatial distribution (Fig.4 a)) The representation of the probability of exceeding
 315 the third quartile (Q3) and not exceeding the first quartile (Q1), allows broad discussion
 316 of the CPI spatial distribution and the identification of hazard clustering (Fig.4 b) and 4
 317 c)). To create distinct classes, reducing the within classes' variance and maximizing the
 318 in-between classes variance, the Jenks natural break classification (Jenks, 1967) was
 319 used, allowing the determination of the best arrangement of values. For the computation,
 320 the Space-Stat Software V. 4.0.18, Biomedwere, was used (Boente et al., 2022,
 321 Albuquerque et al., 2017).

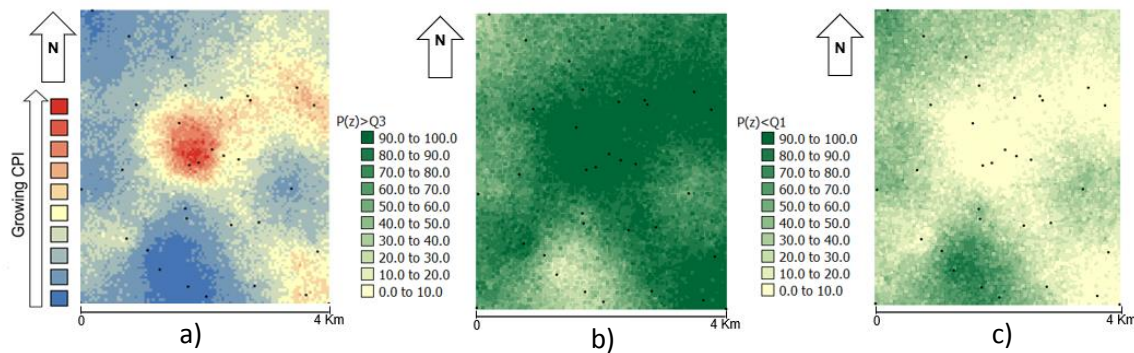


Fig.4. a) SGS average image (MI) b) Probability map of exceeding Q3 and c) Probability map of not exceeding Q1.

The compositional Pollution Indicator (CPI) shows a fair representation of hot spots, especially along the Grândola stream and its tributaries, thereby confirming the larger pollution detected around the old mine tailings and associated waste rock.

4. Conclusions

Geochemical data are compositional data, as the concentrations of elements in any environmental matrix are commonly expressed as parts of a whole and vary together. Once this feature is established, compositional data procedures can be applied to obtain indicators that address pollution, for example, in stream sediment. The method was tested with 33 sediment samples and up to 11 chemical elements from the old Caveira mine in Portugal. Specifically, in the vicinity of the Grândola River and the mine's tailings, the survey revealed a significant risk of contamination. In addition, agriculture is the main focus of economic activities in the region. Two primary courses of action are proposed in light of this:

1. Installation of a surveillance network: The first step is to establish a continuous surveillance and control network in all regions. Setting up a system is necessary to consistently track and assess the levels of contamination in the region. This monitoring would likely involve the installation of sensors for continuous measurement of the PTEs content and a regular collection of in situ samples for validation and to identify any significant changes or deviations.

2. Mitigation strategies for contaminated areas: The second strategy is to focus on the northern region where elevated levels of contamination have been detected. The adverse effects of pollution require the development and implementation of mitigation measures in this region. Efforts to reduce the introduction of contaminants may involve remediation efforts, ecosystem restoration, or changes in local practices.

The survey highlights the interconnectedness of geochemical data and how compositional data procedures can be used to shed light on environmental issues like pollution. It highlights the practical application of these principles through the case study of the Caveira mine area in Portugal, and it emphasizes the importance of addressing contamination risks in a region where agriculture and organic activities are key components of the local economy.

Acknowledgments

The data used in this survey has been presented previously at geoENV2022 in the poster section topic Environmental Pollution and Risk Assessment.

The authors acknowledge the funding provided by the Foundation “LA CAIXA” (Spain) and the Foundation for Science and Technology (FCT) (Portugal), which supported this research through the GeoMatre project: La Caixa/FCT - Project n.º PV20-00006 and, also, the funding provided by the Research Centre for Natural Resources, Environment and Society (CERNAS-IPCB) [project UIDB/00681/2020] funding by Portuguese Foundation for Science and Technology (FCT) and the funding provided by ICT, under contract with FCT (Portuguese Science and Technology Foundation) under the Project FCT—UIDB/04683/2020.

During the preparation of this work, the author(s) used ChatGPT to polish the English, in the conclusions section. After using this tool/service, the author(s) reviewed and edited the content as needed and take(s) full responsibility for the content of the publication.

380 **References**

381 Aitchison, J., 1982. The statistical analysis of compositional data (with discussion). *J. R.*
382 *Stat. Soc. B* 44 (2), 139–177.

383 Aitchison, J., 1986. *The Statistical Analysis of Compositional Data*. Chapman & Hall Ltd.,
384 London (UK) ((Reprinted in 2003 with additional material by The Blackburn Press). 416
385 pp.).

386 Albuquerque, M.T.D., Gerassis, S., Sierra, C., Taboada, J., Martín, J.E., Antunes,
387 I.M.H.R., Gallego, J.R., 2017. Developing a New Bayesian Risk Index for Risk Evaluation
388 of Soil Contamination. *Sci. of the Total Env.*, 603-604, 167-177, DOI:
389 10.1016/j.scitotenv.2017.06.068.

390 Antoniadis, V., Golia, E.E., Shaheen, S.M., Rinklebe, J., 2017. Bioavailability and health
391 risk assessment of potentially toxic elements in Thriasio Plain, near Athens, Greece.

392 Boente, C. Albuquerque, MTD, Gallego, JR, Pawlowsky Glahn, V, Egozcue, JJ, 2022.
393 Compositional Baseline Assessments to Address Soil Pollution: An Application in
394 Langreo, Spain, *Sci. Total Environ.*, ISSN: 0048-9697 Volume: 812, 152383 (12), DOI:
395 10.1016/j.scitotenv.2021.152383.

396 Boente, C., Albuquerque, M.T.D., Fernandez-Brana, A., Gerassis, S., Sierra, C.,
397 Gallego, J.R., 2018. Combining raw and compositional data to determine the spatial
398 patterns of potentially toxic elements in soils. *Sci. Total Environ.* 632–631, 1117–1126.

399 Boente, C., Gerassis, S., Albuquerque, M.T.D., Taboada, J., Gallego, J.R., 2020. Local
400 versus regional soil screening levels to identify potentially polluted areas. *Math. Geosci.*
401 52, 381–396.

402 Boogaart van den, K.G., Tolosana-Delgado, R., 2013. *Analysing Compositional Data*
403 with R. Springer-Verlag, Berlin (258 pp.).

404 Buccianti, A., Grunsky, E., 2014. Compositional data analysis in geochemistry: Are we
405 sure to see what occurs during natural processes? *J. Geochem. Explore.* 141, 1–5.

406 Carvalho, P.C.S., Antunes, I.M.H.R., Albuquerque, M.T.D., Santos, A.C.S., Cunha, P.P.,
407 2022. Stream Sediments as a Repository of U, Th and As Around Abandoned Uranium
408 Mines in Central Portugal: Implications for Water Quality Management. *Env. Earth Sci.*,
409 81, 6, DOI: 0.1007/s12665-022-10275-2.

410 Cicchella, D., Zuzolo, D., Albanese, S., Fedele, L., Tota, D., Guagliardi, Ilaria,
411 Thiombane, Matar, Vivo, Benedetto De, Lima, Annamaria, 2020. Urban soil
412 contamination in Salerno (Italy): Concentrations and patterns of major, minor, trace, and
413 ultra-trace elements in soils. *J. Geochem. Explor.* 213, 106519.

414 Chayes, F., 1962. Numerical correlation and petrographic variation. *J. Geol.* 70 (4), 440
415 452.

416 Chayes, F., 1971. Ratio Correlation. University of Chicago Press, Chicago, IL (USA) (99
417 pp.).

418 Egozcue, J.J., Pawlowsky-Glahn, V., Mateu-Figueras, G., Barceló-Vidal, C., 2003.
419 Isometric log-ratio transformations for compositional data analysis. *Math. Geol.* 35 (3),
420 279–300.

421 Fabian, C., Reimann, C., Fabian, K., Birke, M., Baritz, R., Haslinger, E., 2014. Gemas:
422 spatial distribution of the pH of European agricultural and grazing land soil. *Appl.*
423 *Geochem.* 48, 207–216.

424 Ferreira da Silva, E., Durães N., Reis P., Patinha C., Matos J., Costa M.R., 2015. An
425 integrative assessment of environmental degradation of Caveira. abandoned mine area
426 (Southern Portugal). *Journal of Geochemical Exploration* 159 (2015) 33–47,
427 <http://dx.doi.org/10.1016/j.gexplo.2015.08.004>

428 Filzmoser, P., Hron, K., Reimann, C., 2009. Univariate statistical analysis of
429 environmental (compositional) data: problems and possibilities. *Sci. Total Environ.* 407
430 (23), 6100–6108.

431 Filzmoser, P., Hron, K., 2011. Compositional data analysis: theory and applications. In:
432 Pawlowsky-Glahn, V., Buccianti, A. (Eds.), *Compositional Data Analysis: Theory And*
433 *Applications*. John Wiley & Sons, pp. 59–72.

434 Filzmoser, P., Hron, K., Martín-Fernández, J., Palarea-Albaladejo, J., 2021. *Advances in*
435 *Compositional Data Analysis: Festschrift in Honour of Vera Pawlowsky-Glahn*. Springer
436 International Publishing.

437 Goovaerts, P., 1997. *Geostatistics for Natural Resources Evaluation*. Applied
438 Geostatistics Series. Oxford University Press, New York, NY (USA) (483 pp.).

439 Hakanson, L., 1980. An Ecological Risk Index for Aquatic Pollution Control A
440 Sedimentological Approach. *Water Research*, 14, 975-1001.,
441 Buccianti [http://dx.doi.org/10.1016/0043-1354\(80\)90143-8](http://dx.doi.org/10.1016/0043-1354(80)90143-8)

442 Jenks, G.F., 1967. The data model concept in statistical mapping. International Yearbook
443 of Cartography. 7, pp. 186–190.

444 Journel, A.G., Huijbregts, C.J., 1978. Mining Geostatistics. Academic Press, London
445 (UK) (600 pp.).

446 Kowalska, J.B., Mazurek, R., Gasiorek, M., Zaleski, T., 2018. Pollution indices as useful
447 tools for the comprehensive evaluation of the degree of soil contamination: a review.
448 Environ. Geochem. Health 40, 2395–2420.

449 Kumuduni, N. P., Sabry M. S., Season S. C., Daniel C.W. T., Yohey H., Deyi H., Nanthi
450 S. B., Jörg R., Yong S. O., 2020. Soil amendments for immobilization of potentially toxic
451 elements in contaminated soils: A critical review. Environment International 134 (2020)
452 105046, <https://doi.org/10.1016/j.envint.2019.105046>.

453 Langella O, Valot B, Jacob D, Balliau T, Flores R, Hoogland C, Joets J, Zivy M (2013)
454 Management and dissemination of MS proteomic data with PROTICdb: example of a
455 quantitative comparison between methods of protein extraction, Proteomics. 2013
456 May;13(9):1457-66.

457 Matheron, G. 1971. The Theory of Regionalized Variables and Its Applications. Les
458 Cahiers du Centre de Morphologie Mathématique in Fontainebleau, Paris.

459 Martins, L., Oliveira, D., 2000. Exploration and Mining. Instituto Geológico e Mineiro,
460 Lisboa (20 pp.).

461 McKinley, J.M., Hron, K., Grunsky, E.C., Reimann, C., de Caritat, P., Filzmoser, P., van
462 den Boogaart, K.G., Tolosana-Delgado, R., 2016. The single-component geochemical
463 map: fact or fiction? J. Geochem. Explor. 162, 16–28.

464 Muller, G., 1969. Index of geoaccumulation in sediments of the Rhine River. Geol. J. 2,
465 108–118.

466 Mullineaux, S.T., McKinley, J.M., Marks, N.J., Scantlebury, D.M., Doherty, R., 2021.
467 Heavy metal (pte) ecotoxicology, data review: traditional vs. a compositional approach.
468 Sci. Total Environ. 769 (14524), 6. (378 pp.)

469 Pawlowsky-Glahn, V., Buccianti, A. (Eds.), 2011. Compositional Data Analysis: Theory
470 and Applications. John Wiley & Sons.

471 Pawlowsky-Glahn, V., Serra, J. (Eds.), 2019. Matheron's Theory of Regionalised
472 Variables. Oxford University Press (208 pp.).

473 Pawlowsky-Glahn, V., Egozcue, J.J., Tolosana-Delgado, R., 2015. Modeling and
474 analysis of compositional data. *Statistics in Practice*. John Wiley & Sons, Chichester UK
475 (272 pp.).

476 Pawlowsky-Glahn, V., Egozcue, J.J., 2001. A geometric approach to statistical analysis
477 on the simplex. *Stoch. Environ. Res. Risk Assess.* 15 (5), 384–398.

478 Petrik, A., Thiombane, M., Lima, A., Albanese, S., Buscher, J.T., De Vivo, B., 2018. Soil
479 contamination compositional index: a new approach to quantify contamination
480 demonstrated by assessing compositional source patterns of potentially toxic elements
481 in the Campania region (Italy). *J. Appl. Geochem.* 96, 264–276.

482 Rivoirard, J., 2005. Concepts and methods of geostatistics. Space, structure, and
483 randomness. In: Meyer, F., Schmitt, M. (Eds.), *Contributions in Honor of Georges
484 Matheron in the Fields of Geostatistics, Random Sets, and Mathematical Morphology*,
485 Bilodeau (ISBN: 978-0-387-20331-7).

486 Sucharova, J., Suchara, I., Hola, M., Marikova, S., Reimann, C., Boyd, R., Filzmoser, P.,
487 Englmaier, P., 2012. Top-/bottom-soil ratios and enrichment factors: What do they show?
488 *J. Appl. Geochem.* 27, 138–145

489 Tepanosyan, G., Sahakyan, L., Maghakyan, N., Saghatelyan, A., 2020. Combination of
490 compositional data analysis and machine learning approaches to identify sources and
491 geochemical associations of potentially toxic elements in soil and assess the associated
492 human health risk in a mining city. *Environ. Pollut.* 261, 11421.

493 Wang, Z., Chen, X., Yu, D., Zhang, L., Wang, J., Lv, J., 2021. Source apportionment and
494 spatial distribution of potentially toxic elements in soils: a new exploration on receptor
495 and geostatistical models. *Sci. Total Environ.* 759 (14342), 8.

496 Wei, Y., Wang, Z., Wang, H., Yao, T., Li, Y., 2018. Promoting inclusive water governance
497 and forecasting the structure of water consumption based on compositional data: a case
498 study of Beijing. *Sci. Total Environ.* 634, 407–416.

499 Wilkinson L, Friendly M (2009) The history of the cluster heat map. *Am Stat* 63(2):179–
500 184. <https://doi.org/10.1198/tas.2009.0033>

Table 1. Element concentrations in the stream sediment samples (spring season) from Grândola, and its tributary streams. These waterways belong to Sado watershed.

Samples * (mg/Kg)	As	Cd	Co	Cr	Mn	Ni	V	Zn	Al	Fe	Pb	Hg	pH (H ₂ O)
CV1	234,9	1,5	0,4	2,3	16,9	1,6	3,3	94,2	1441,6	10217,0	38458,7	127,9	2,30
CV2	238,6	< 0,5	0,4	1,6	24,5	1,0	2,0	96,4	2168,4	17815,8	29837,2	78,2	2,06
CV3	517,6	< 0,5	0,8	1,5	99,6	0,9	2,9	122,3	16128,4	65825,8	13775,3	125,8	4,57
CV4	< 1,5	< 0,5	3,9	13,3	172,7	10,3	14,3	36,4	18321,3	31828,4	51,2	1,7	6,61
CV5	14,7	< 0,5	3,5	15,6	261,9	12,7	15,5	47,2	13099,4	27183,4	2881,5	13,7	6,00
CV6	< 1,5	< 0,5	3,4	17,6	208,4	9,3	24,3	30,0	26272,6	21172,3	221,4	0,2	6,54
CV7	< 1,5	< 0,5	4,2	18,6	399,1	11,2	29,2	36,4	29376,6	28193,2	97,2	0,6	6,64
CV8	< 1,5	< 0,5	4,6	19,5	455,6	12,3	25,7	37,5	24811,4	28361,9	15,0	0,3	7,17
CV9	< 1,5	< 0,5	5,8	13,4	414,1	12,4	13,8	34,7	13007,8	27207,6	16,4	0,2	4,99
CV10	< 1,5	< 0,5	5,6	15	315	21,6	22,9	46,3	23727,5	23919,7	18,2	0,6	5,12
CV11	3,4	< 0,5	1,0	1,4	148	1,2	2,6	15,8	8807,1	12058,1	21,5	0,3	5,05
CV12	31,2	< 0,5	4,2	9,6	138,6	10,6	15,9	140,4	11176,5	29630,2	92,7	2,6	5,30
CV13	1,6	< 0,5	34,4	23,8	903	21,8	36,4	165,8	44359,5	42371,5	36,3	1,6	7,29
CV14	1,6	< 0,5	4,1	16,1	434,9	15,9	24,3	47,5	18683,1	21463,1	36,6	0,6	6,03
CV15	1,7	< 0,5	0,5	1,9	82,2	0,6	3,6	5,3	8882,1	3720,9	2,5	0,2	5,48
CV16	< 1,5	< 0,5	0,6	2,1	198,2	1,3	4,6	17,5	4821,9	5337,6	25,9	0,2	5,98
CV17	4,0	< 0,5	1,6	4,3	412,9	4,0	5,2	15,8	10396,1	16746,8	27,1	0,1	6,35
CV18	< 1,5	< 0,5	0,6	2,5	117,3	1,5	2,7	8,9	3475,2	3540,5	8,1	0,3	5,51
CV19	1,8	< 0,5	0,5	1,4	66,3	0,7	2,3	8,1	3044,8	3855,6	7,6	0,1	5,55
CV20	2,1	< 0,5	1,0	4,5	169,6	1,5	6,8	10,6	3677	5856,6	9,8	0,2	5,82
CV21	< 1,5	< 0,5	0,8	2,0	194,6	0,5	3,6	9,9	3574,9	3936,7	7,9	0,1	6,04
CV23	1,9	< 0,5	1,3	11,9	98,5	6,2	14,1	136,3	9503,4	9550,3	38,1	3,0	7,39
CV24	44,2	< 0,5	1,5	7,0	79,2	5,8	12,1	122,4	9728,8	13370,1	585,3	5,7	6,74
CV25	< 1,5	< 0,5	0,4	1,5	84,8	0	3,7	6,3	14787,2	7836,1	4,4	0,1	6,63
CV26	140,3	< 0,5	0,4	1,6	34,4	2,0	2,6	123,4	1193,7	10730,9	44540,5	46,8	2,34
CV27	32,3	< 0,5	3,6	11,6	177,5	12,5	17,9	129,0	13208,0	25540,5	82,8	7,3	6,39
CV28	< 1,5	< 0,5	3,7	16	385,5	10,1	24,6	36,0	22281,1	17596,5	29,1	1,3	5,34
CV29	< 1,5	< 0,5	3,9	18,4	394,6	10,7	25,6	36,2	22665,1	18556,6	14,5	0,2	6,82
CV30	< 1,5	< 0,5	4,1	13,8	258,4	11,8	15,9	39,8	11984,7	19370,5	21,5	0,1	6,16
CV31	9,0	< 0,5	2,1	14,2	106,4	10,5	15,7	30,2	6909,5	23545,1	31,0	0,2	6,21
CV32	30,8	< 0,5	3,4	15,7	291,3	8,9	24,6	88,6	24220,0	19152,6	107,7	2,3	6,57
CV33	265,2	< 0,5	3,9	9,3	422,5	8,6	11,6	108,2	11998,7	30136,3	88,8	1,6	4,26
CV34	748,2	< 0,5	0,4	8,3	77,6	3,9	10,8	161,8	6854,4	44363,4	23162,4	381,4	2,13

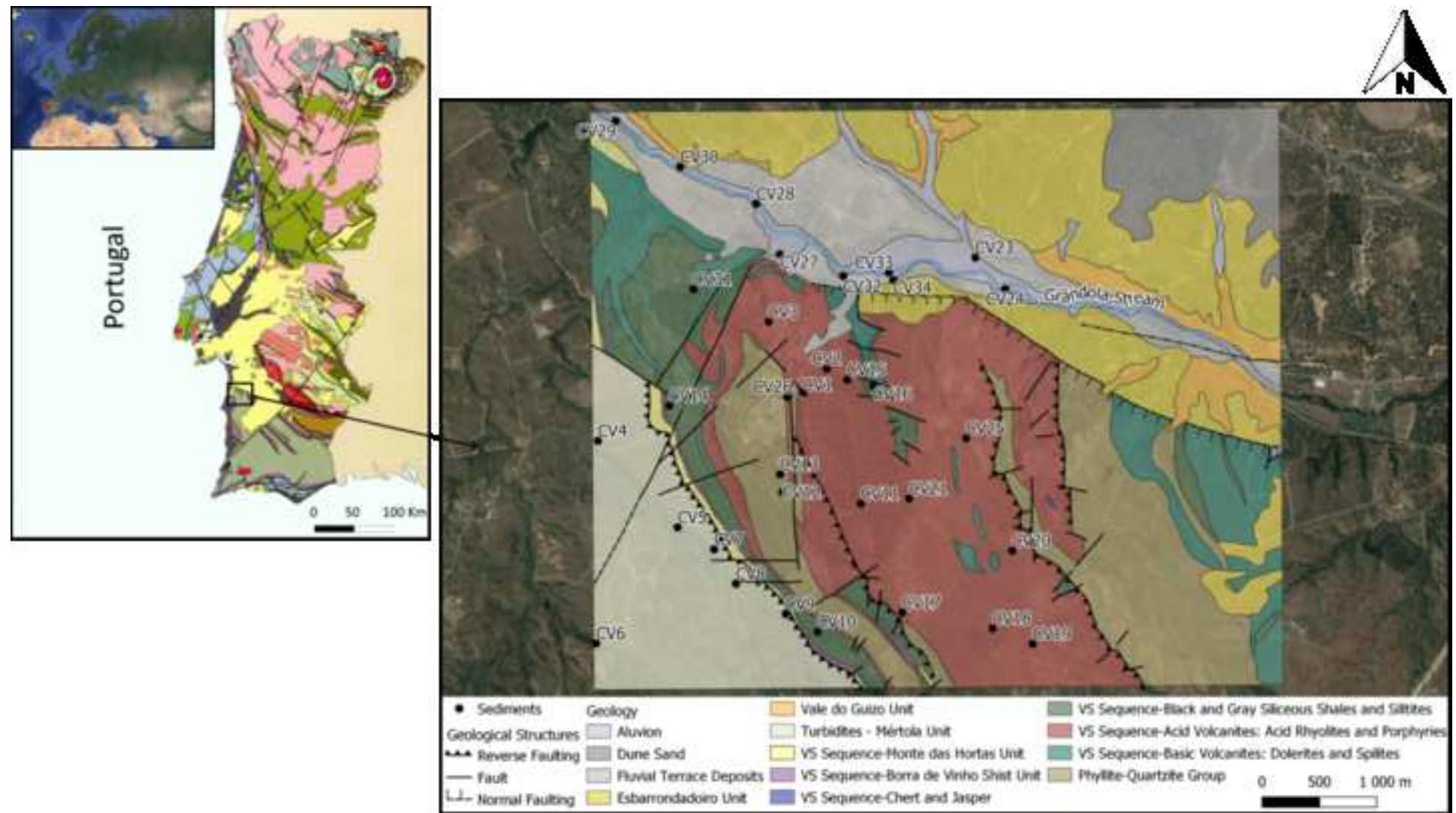
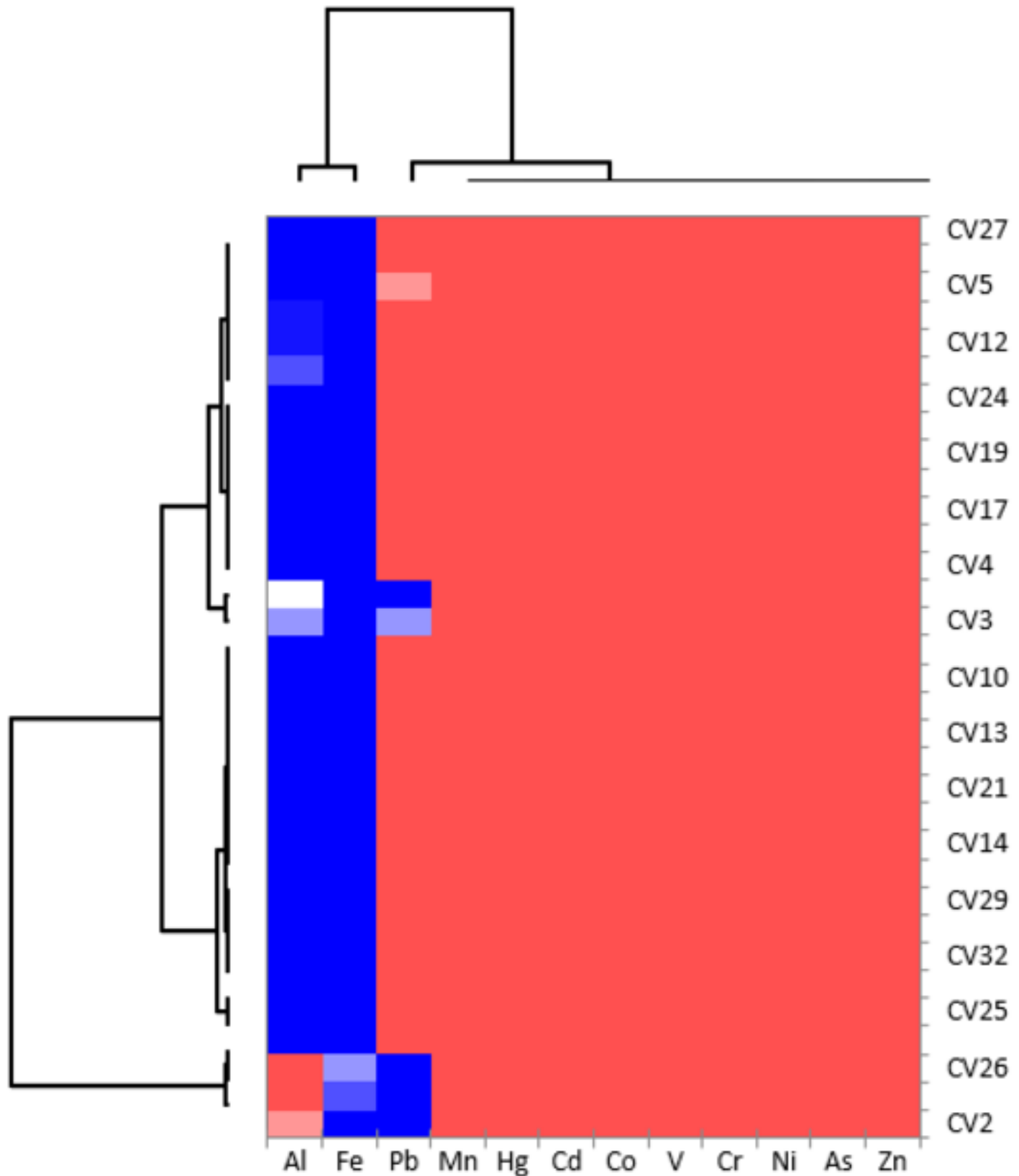


Figure2

[Click here to access/download;Figure;Fig.2.PNG](#)



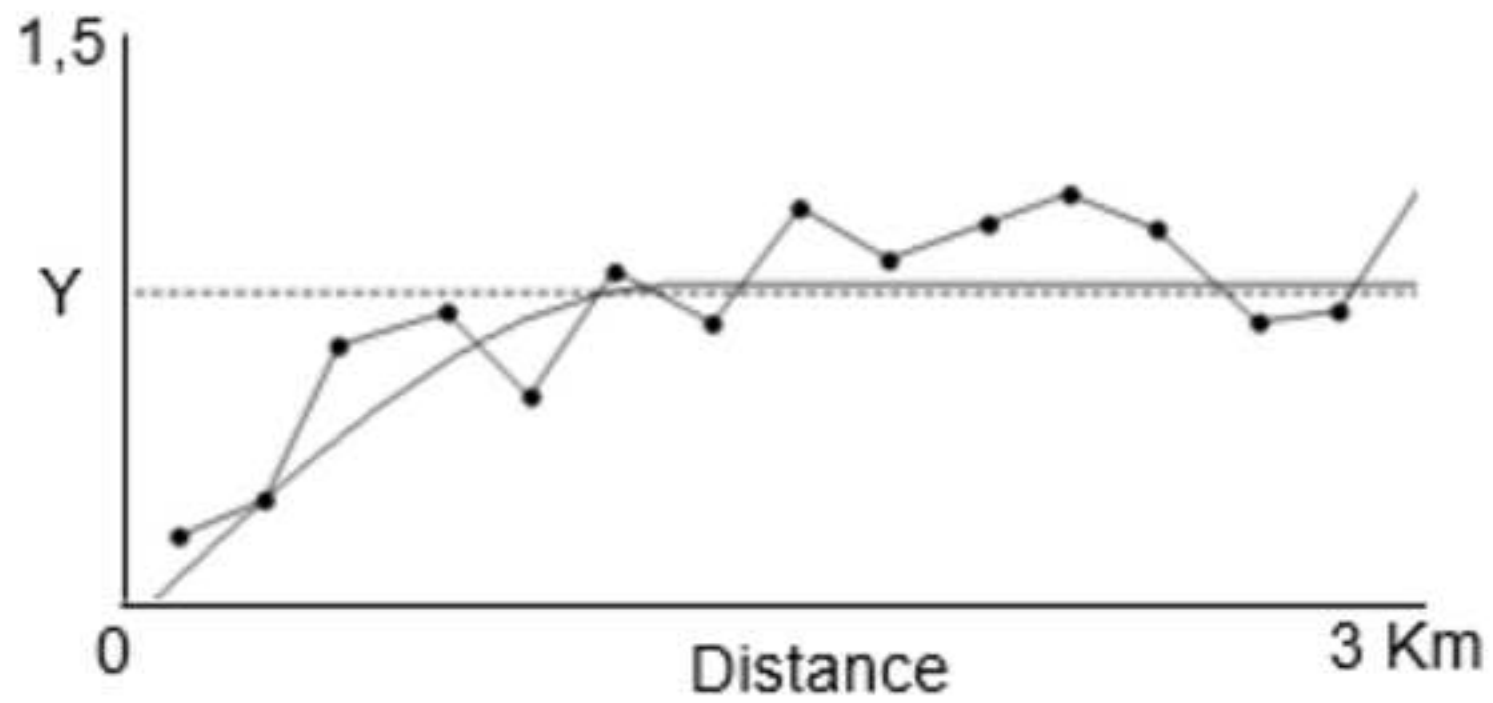
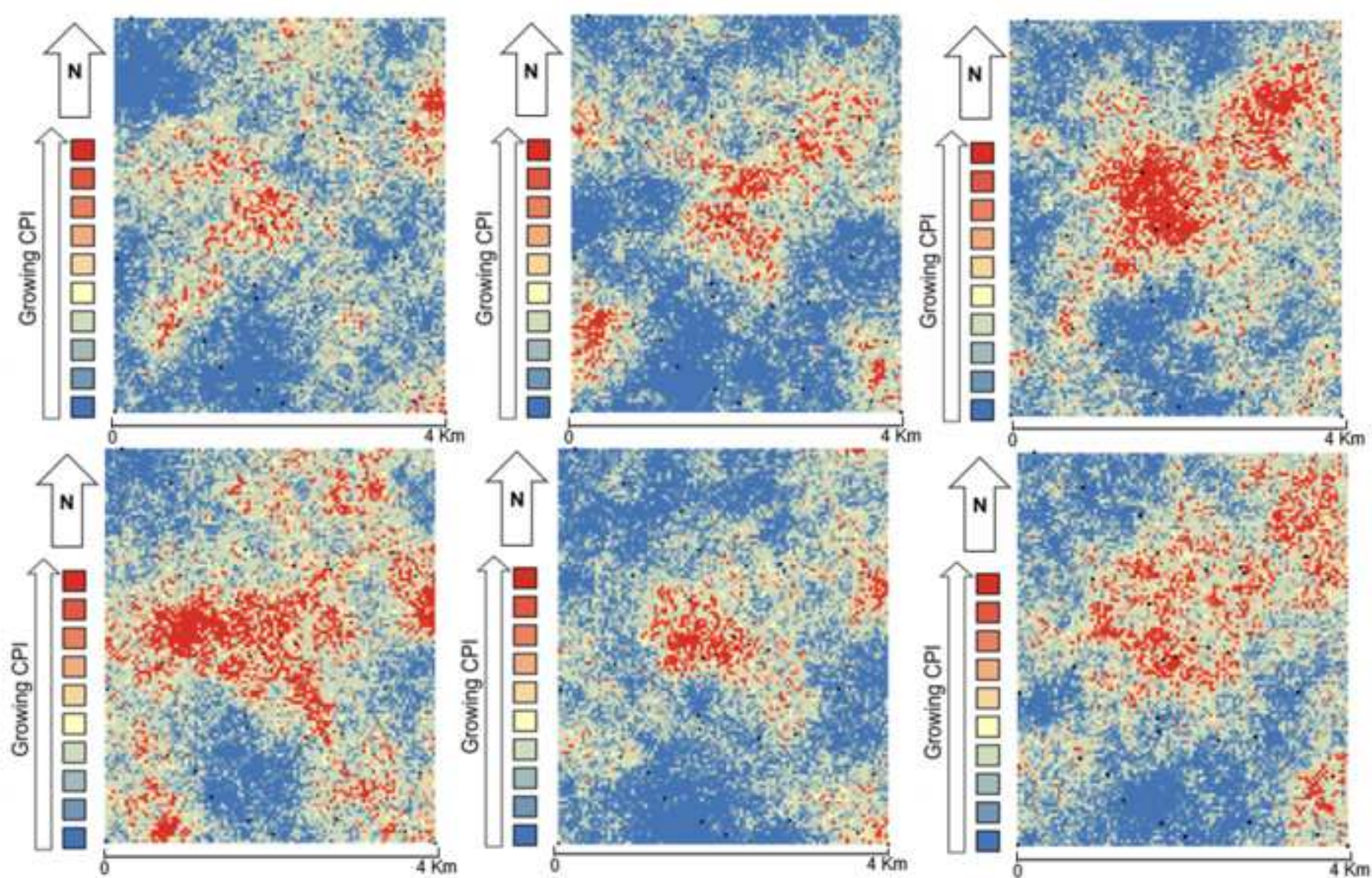
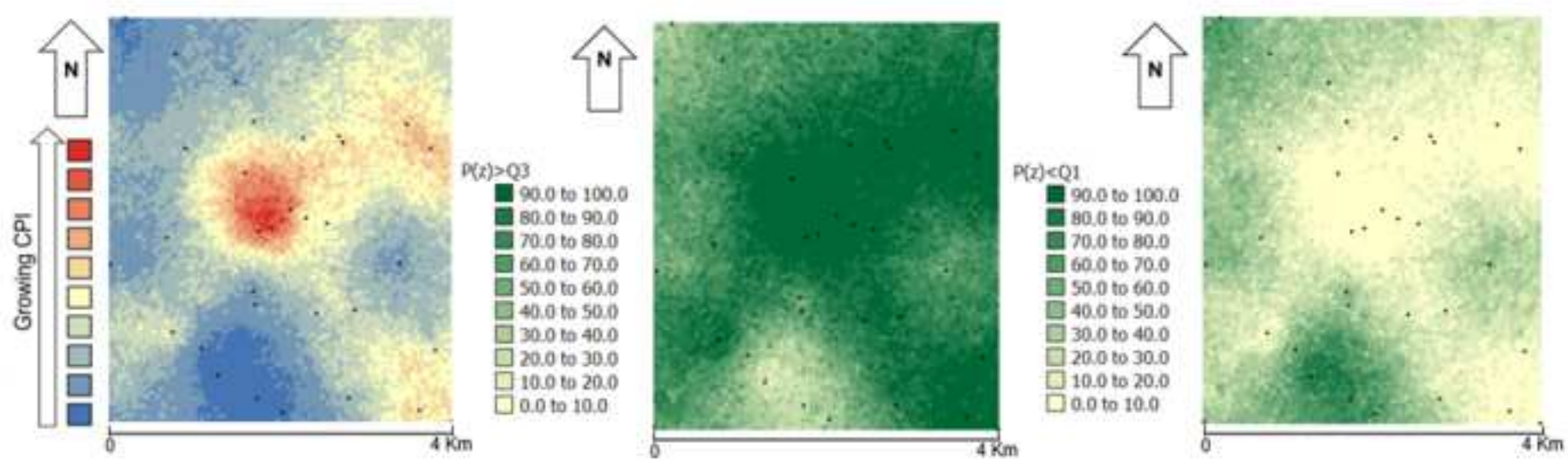


Figure4

[Click here to access/download;Figure;Fig.4.PNG](#)





Click here to access/download
Supplementary Material
Supplementary Material.docx

Declaration of interests

The authors declare that they have no known competing financial interests or personal relationships that could have appeared to influence the work reported in this paper.

The authors declare the following financial interests/personal relationships which may be considered as potential competing interests:

1
2
3
4
5
6
7
8
9
10
11
12
13
14
15
16
17
18
19
20
21
22
23
24
25
26
27
28
29
30
31
32
33
34
35
36
37
38
39
40
41
42
43
44
45
46
47
48
49

Soil Pollution?
Pollutants - As, Zn, Pb and Hg
+
Non-Pollutants – Al and Fe



Definition of a baseline for soil pollution assessment in the Caveira Mine, Portugal



First Step
Defining the Compositional Pollution Indicator (CPI): Expert based criteria

$$CPI = K \log \left(\frac{gm(As \ Zn \ Pb \ Hg)}{gm(Al \ Fe)} \right)$$

gm stands for geometrical mean and K for normalization constant

Second Step

A hundred Sequential Gaussian Simulations and the Probability maps of exceeding the Q3 and not exceeding the Q1

